Interface-selected waves and their influence on wave competition

Xiaohua Cui,[1] Xiaoqing Huang,[1] Zhoujian Cao,[2] Hong Zhang,[3] and Gang Hu[1,*]
[1]*Department of Physics, Beijing Normal University, Beijing 100875, China*
[2]*Institute of Applied Mathematics, Academy of Mathematics and System Science, Chinese Academy of Sciences, Beijing 100080, China*
[3]*Zhejiang Institute of Modern Physics and Department of Physics, Zhejiang University, Hangzhou 310027, China*
(Received 22 August 2007; revised manuscript received 19 June 2008; published 4 August 2008)

In this paper we study nonlinear oscillatory systems consisting of two media, one supporting forward propagating waves and the other inwardly propagating waves, separated by an interface. We find that the interface can select the type of wave. Under certain well-defined parameter condition, these waves propagate in two different media with the same frequency and same wave number; the interface of the two media is transparent to these waves. The frequency and wave number of these interface-selected waves (ISWs) are predicted explicitly. When parameters are varied from this parameter set, the wave numbers of the two domains become different, and the difference increases from zero continuously as the distance between the given parameters and this parameter set increases from zero. It is found that ISWs can play crucial roles in practical problems of wave competition, e.g., ISWs can suppress spirals and antispirals.

DOI: 10.1103/PhysRevE.78.026202 PACS number(s): 05.45.−a, 47.54.−r, 04.30.Nk

The behavior of waves around interfaces between two media have attracted continual and great interest [1–7]. In linear optics we are familiar with the problems of wave reflection and refraction, which are predicted analytically. However, for nonlinear systems the interface-related behaviors become much more complex and diverse, and much less known.

The problems of wave propagation in linear and nonlinear media have also attracted considerable attention. Recently, new observations of inwardly propagating waves have stimulated considerable interest in this field. For several centuries, scientists have known waves propagating only forward from the wave source, called normal waves (NWs). In recent years, different types of waves propagating toward the wave source [called here antiwaves (AWs)] have been observed in both linear optics [1,8] and nonlinear oscillatory systems [9–14]. These phenomena introduce completely new topics of the interface problem. For instance, the phenomenon of negative refraction has been reported in both linear optics [1,8] and nonlinear oscillatory systems [3,7].

In the present paper, we find another nonlinear interface phenomenon: the interface of two different media can generate waves, called here interface-selected waves (ISWs). On a well-defined parameter surface the frequency and wave number (also wavelength) of ISWs are identical in two media with different parameters, and they can be predicted analytically. Away from but near this surface ISWs still exist, although the above analytical predictions are no longer available and the wave numbers of ISWs in the two domains are no longer identical. When parameters are varied away from this surface continuously, wave numbers change continuously, and the difference are varied of wave numbers in the two domains also increases from zero continuously. It is found that ISWs play crucial roles in practical problems of wave competition in oscillatory systems, e.g., in suppressing spirals and antispirals.

*ganghu@bnu.edu.cn

We consider the following bidomain reaction-diffusion system:

$$\frac{\partial \mathbf{U}_1}{\partial t} = \mathbf{f}(\mathbf{U}_1, \boldsymbol{\mu}_1, \boldsymbol{\nu}_1) + \mathbf{D}(\boldsymbol{\gamma}_1)\,\nabla^2 \mathbf{U}_1, \tag{1a}$$

$$\frac{\partial \mathbf{U}_2}{\partial t} = \mathbf{f}(\mathbf{U}_2, \boldsymbol{\mu}_2, \boldsymbol{\nu}_2) + \mathbf{D}(\boldsymbol{\gamma}_2)\,\nabla^2 \mathbf{U}_2, \tag{1b}$$

$$\mathbf{U}_i = (U_i^{(1)}, \ldots, U_i^{(m)}), \quad \boldsymbol{\mu}_i = (\mu_i^{(1)}, \ldots, \mu_i^{(p)}),$$

$$\boldsymbol{\nu}_i = (\nu_i^{(1)}, \ldots, \nu_i^{(q)}), \quad \boldsymbol{\gamma}_i = (\gamma_i^{(1)}, \ldots, \gamma_i^{(l)}),$$

$$i = 1,2, \quad m \geqslant 2,$$

where $\mathbf{D}(\boldsymbol{\gamma}_i)$ is an $m \times m$ matrix with constant elements depending on $\boldsymbol{\gamma}_i$. The function $\mathbf{f}$ and diffusion matrix $\mathbf{D}$ in the two domains are identical because the same reaction-diffusion processes occur in both sides. On the other hand, the dynamical evolutions in each side may be different due to different control parameters $(\boldsymbol{\mu}_1, \boldsymbol{\nu}_1, \boldsymbol{\gamma}_1)$ and $(\boldsymbol{\mu}_2, \boldsymbol{\nu}_2, \boldsymbol{\gamma}_2)$. We represent the interface between the two domains by I; then the following boundary conditions are required on I:

$$\mathbf{U}_{1\{I\}} = \mathbf{U}_{2\{I\}}, \quad \frac{\partial \mathbf{U}_1}{\partial n_{\{I\}}} = \frac{\partial \mathbf{U}_2}{\partial n_{\{I\}}}, \tag{2}$$

where $\partial \mathbf{U}_i / \partial n_{\{I\}}$ indicates a derivative of $\mathbf{U}_i$ over space variable along the direction perpendicular to the interface I. We assume that $\mathbf{U}_1 = \mathbf{U}_2 = \mathbf{0}$ is a stable point of Eq. (1) and $\boldsymbol{\mu}_i(\boldsymbol{\nu}_i)$ controls (does not control) the linear terms of $\mathbf{U}_i$ for the reaction parts. A Hopf bifurcation with frequency ω_0 is supposed to occur at parameters $\boldsymbol{\mu}_1 = \boldsymbol{\mu}_2 = \boldsymbol{\mu}_0$. Moreover, we assume further that both $\boldsymbol{\mu}_1$ and $\boldsymbol{\mu}_2$ are slightly beyond the Hopf bifurcation point,

$$\sum_{j=1}^{p} (\mu_i^{(j)} - \mu_0^{(j)})^2 \ll 1, \quad i = 1,2. \tag{3}$$

At $\boldsymbol{\mu}_i$, $\mathbf{U}_i$ performs periodic oscillations of frequency ω_i, and ω_i approaches ω_0 as $\boldsymbol{\mu}_i$ is reduced to $\boldsymbol{\mu}_0$ $(i=1,2)$. Under condition (3) Eq. (1) can be reduced to amplitude equations, i.e., the bidomain complex Ginzburg-Landau equations (BCGLEs) by the approach standard for the derivative of single-domain CGLEs [15,16]:

$$\frac{\partial A_1}{\partial t} = a_1(1 - i\Omega_1)A_1 - b_1(1 + i\alpha_1)|A_1|^2 A_1 + c_1(1 + i\beta_1)\nabla^2 A_1, \tag{4a}$$

$$\frac{\partial A_2}{\partial t} = a_2(1 - i\Omega_2)A_2 - b_2(1 + i\alpha_2)|A_2|^2 A_2 + c_2(1 + i\beta_2)\nabla^2 A_2, \tag{4b}$$

$$A_{1\{I\}} = A_{2\{I\}}, \quad \frac{\partial A_1}{\partial n_{\{I\}}} = \frac{\partial A_2}{\partial n_{\{I\}}}, \tag{4c}$$

where (a_i, Ω_i), (b_i, α_i), and (c_i, β_i) are related to $\boldsymbol{\mu}_i - \boldsymbol{\mu}_0$ $(\boldsymbol{\mu}_i - \boldsymbol{\mu}_0, \nu_i)$, and $(\boldsymbol{\mu}_i - \boldsymbol{\mu}_0, \boldsymbol{\gamma}_i)$, respectively. The continuity conditions Eq. (4c) can be derived from condition (2) because the transformation from U_1 to A_1 is exactly the same as that from U_2 to A_2 (in the two domains, the amplitude equations are derived at a common Hopf bifurcation point with an identical linear matrix at $\boldsymbol{\mu}_0$), and the transformations from U_i to A_i $(i=1,2)$ are determined only by this linear matrix. In Eq. (4) A_1 and A_2 are complex variables on each side of the interface. With scaling transformations we can fix a_1, b_1, c_1, and Ω_1, and the remaining eight parameters are irreducible for BCGLE systems. In the following study we will set $a_1 = b_1 = c_1 = 1$, $\Omega_1 = 0$ for numerical simulations unless specified otherwise and all the theoretical formulas are given generally for 12 parameters. Without the interface interaction, the two media have their single-domain planar wave solutions [2,17]

$$A_i(x,t) = \sqrt{\left(\frac{1}{b_i}(a_i - c_i k_i^2)\right)} e^{i(k_i x - \omega_i t)}, \quad 0 \leqslant k_i^2 \leqslant \frac{a_i}{c_i}, \tag{5a}$$

$$\omega_i = a_i(\alpha_i + \Omega_i) + c_i(\beta_i - \alpha_i)k^2, \quad a_i, b_i, c_i > 0. \tag{5b}$$

Waves in media M_1 and M_2 are classified as NWs and AWs under the conditions [3,12,14]

$$\omega_i a_i(\Omega_i + \alpha_i) < 0; \quad \text{or,} \quad \omega_i a_i(\Omega_i + \alpha_i) > 0 \quad \text{and} \quad |\omega_i| > |a_i(\Omega_i + \alpha_i)| \quad \text{(NWs)}, \tag{6a}$$

$$\omega_i a_i(\Omega_i + \alpha_i) > 0 \quad \text{and} \quad |\omega_i| < |a_i(\Omega_i + \alpha_i)| \quad \text{(AWs)}. \tag{6b}$$

By AWs we mean waves with negative phase velocity, while both NWs and AWs have positive group velocities [11,12,14]. Now we focus on the interface-related problems, and start from a one-dimensional (1D) BCGLE system. We are interested in how the interface can significantly influence the system dynamics. In Figs. 1(a)–1(c) we study the system evolution at two different parameter sets with random initial conditions, and find characteristically different features in the asymptotic states. The most significant observation is given in Figs. 1(a) and 1(b), where we find homogeneous planar waves moving in both media from right to left with a constant velocity and transparently crossing the interface. These homogeneous running waves originate from the interface [see Fig. 1(b)] and, therefore are called interface selected waves. The phenomenon of Fig. 1(a) is surprising. With two media having different control parameters we intuitively expect that the waves in the two media must have different wave numbers (even if both sides may have the same frequency). This common feature is clearly seen in Fig. 1(c), where we observe uniform bulk oscillation in the right medium and waves propagating from left to right in the left medium, clearly manifesting the interface *I*. However, in Fig. 1(a) waves propagate seemingly in a homogeneous medium without experiencing any difference between M_1 and M_2; the interface is transparent to the waves. Moreover, the realization of these running waves is stable against different initial perturbations. This characteristic phenomenon can never exist in linear systems, and has not been observed so far in nonlinear systems to our knowledge.

It is interesting that we can predict the frequency and wave number of ISWs explicitly and exactly under certain parameter conditions. For the case of Fig. 1(a) we can determine the frequency and wave number by the following simple requirements:

$$\omega_1(k_1) = \omega_2(k_2), \quad k_1 = k_2, \quad |A_1| = |A_2|. \tag{7}$$

Inserting Eqs. (7) into Eq. (5), we obtain a unique set of solutions ω_I, k_I:

$$k_1^2 = k_2^2 = k_I^2 = \frac{a_1(\alpha_1 + \Omega_1) - a_2(\alpha_2 + \Omega_2)}{c_2(\beta_2 - \alpha_2) - c_1(\beta_1 - \alpha_1)}, \tag{8a}$$

$$\omega_1 = \omega_2 = \omega_I = \frac{a_1(\alpha_1 + \Omega_1)c_2(\beta_2 - \alpha_2) - c_1(\beta_1 - \alpha_1)a_2(\alpha_2 + \Omega_2)}{c_2(\beta_2 - \alpha_2) - c_1(\beta_1 - \alpha_1)}, \tag{8b}$$

and these solutions are exact in the parameter surface,

$$\text{for } c_1b_2 - c_2b_1 \neq 0 \quad \text{if and only if } \frac{a_1b_2 - a_2b_1}{c_1b_2 - c_2b_1} - \frac{a_1(\alpha_1 + \Omega_1) - a_2(\alpha_2 + \Omega_2)}{c_2(\beta_2 - \alpha_2) - c_1(\beta_1 - \alpha_1)} = 0,$$

$$\text{for } c_1b_2 - c_2b_1 = 0 \quad \text{if and only if } a_1b_2 - a_2b_1 = 0, \tag{8c}$$

which is obtained by inserting Eq. (8a) into Eq. (5a), and by identifying $|A_1|=|A_2|$. It can be easily confirmed that on the parameter surface Eq. (8c) the planar wave solution Eq. (5) with frequency and wave numbers given by Eqs. (8a) and (8b) are exact solutions of the BCGLE. Moreover, the predictions of Eqs. (7) and (8a)–(8c) agree exactly with the numerical results of Fig. 1(a).

In Figs. 2(a) and 2(b) we specify the surface of Eq. (8c) in some parameter planes, where the solid lines represent the parameters satisfying conditions (8c). In Figs. 2(c) and 2(d) we vary parameters along the solid line of Fig. 2(a) and numerically compute the 1D BCGLEs. we compare the numerical results (empty circles and triangles) with the theoretical predictions of Eqs. (8a) and (8c) (solid lines), and find (i) ISWs exist in a large area of surface Eq. (8c); (ii) the predictions of Eqs. (8a) and (8b) coincide with the numerical results exactly (within computation precision). In Fig. 2(e) we fix a parameter set on the surface (black disk T) and present the asymptotic pattern evolution of the BCGLE system. It is clearly shown that ISWs, with the wave number and frequency predicted by Eqs. (8a) and (8b), asymptotically control the entire bidomain during their propagation. To demonstrate the possibility of observation of ISWs in experiments, we study a reaction-diffusion model: the bidomain Brusselator. In Fig. 2(f), we show ISWs of this chemical model, satisfying all conditions of Eqs. (7).

The solutions of Eqs. (8a) and (8b) are exact for BCGLE only on the parameter surface of Eq. (8c). Slightly away

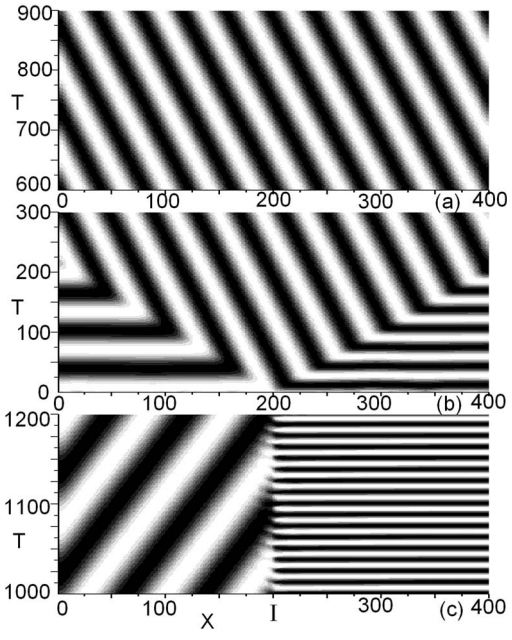

FIG. 1. (a)–(c) Contour patterns of ReA_i of a 1D BCGLE system with interface I. Domains M_i $(i=1,2)$ have length L and parameters α_i, β_i, and $a_i=b_i=c_i=1$, $\Omega_i=0$, $i=1,2$. Numerical simulations are made with space step $dx=0.5$, time step $dt=0.005$, and $L=200$. No-flux boundary condition, randomly chosen initial conditions, and the above time and space steps are used in all figures for numerical simulations unless specified otherwise. (a) $\alpha_1=0.1$, $\beta_1=-1.4$, $\alpha_2=-0.2$, $\beta_2=1.4$. Interface-selected waves homogeneous in M_1 and M_2 are observed, and the interface is transparent to ISWs. (b) The same as (a) with early time evolution plotted. It is clearly shown that ISWs originate from the interface. (c) $\alpha_1=0.1$, $\beta_1=-1.4$, $\alpha_2=0.5$, $\beta_2=1.4$. M_1 and M_2 support different regular waves, clearly manifesting interface I.

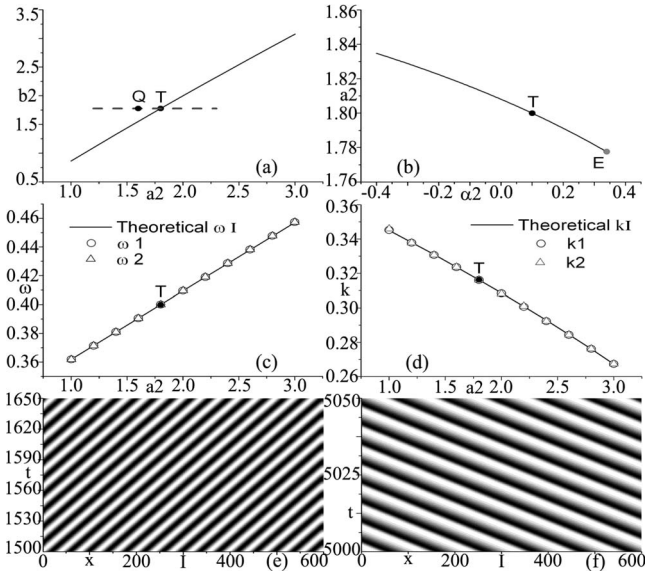

FIG. 2. (a) Surface Eq. (8c) (solid line) plotted in a_2-b_2 plane with $\Omega_2=0$, $c_2=2.0$, $\alpha_1=0.6$, $\beta_1=-1.4$, $\alpha_2=0.1$, $\beta_2=1.2$. (b) The same as (a) with surface (8c) plotted in α_2-a_2 plane, $b_2=1.778$. Point E corresponds to the boundary $k^2=0$. (c) Frequency of ISWs that are selected along the solid line of (a). The theoretical prediction Eq. (8a) (solid line) coincides with numerical simulation for 1D BCGLE (empty circles and triangles) perfectly. (d) The same as (c) with wave numbers $k_1=k_2$ plotted. Agreement between theoretical prediction Eq. (8a) and numerical results is confirmed. (e) ISW pattern obtained by using the parameter set $a_2=1.8$, $b_2=1.778$ [point T in (a)]. (f) The same as (e) with contour pattern of variable v of reaction-diffusion system of Brusselator which is numerically computed for a 1D chain. The system is $\partial u_i/\partial t=a_i-(b_i+1+\gamma_i)u+(1+\sigma_i)u^2v+\delta_{ui}\nabla^2u$, $\partial v_i/\partial t=b_iu-(1+\sigma_i)u^2v+\delta_{vi}\nabla^2v$, $i=1,2$, $a_1=1.0$, $b_1=2.24$, $\gamma_1=\sigma_1=0.0$, $\delta_{u1}=2.31$, $\delta_{v1}=2.17$; $a_2=1.02$, $b_2=2.2624$, $\gamma_2=0.02$, $\sigma_2=0.01$, $\delta_{u2}=0.95$, $\delta_{v2}=2.47$; $dx=dy=0.5$, $dt=0.0025$, $L=300$. ISWs with identical w and k are observed.

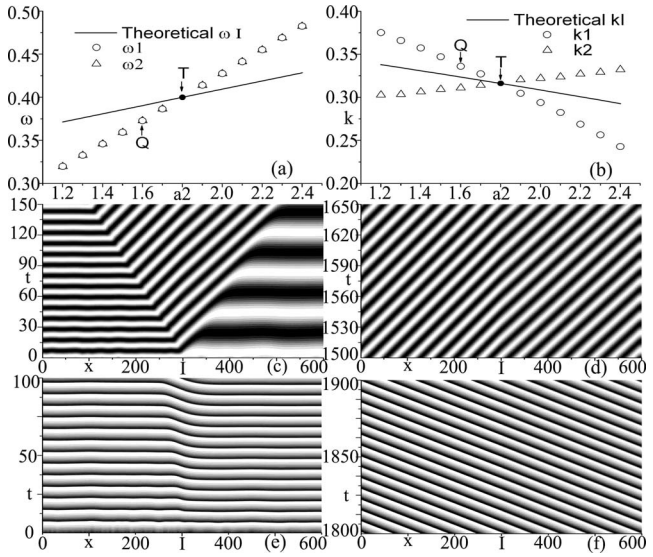

FIG. 3. (a),(b) The same as Figs. 2(c) and 2(d), respectively, with parameters varied along the dashed line of Fig. 2(a). Numerical simulations are made for 1D BCGLE. Now deviations between theoretical results of Eqs. (8a) and (8b) and the numerical results are observed. Deviation increases as parameters vary away from the surface Eq. (8c). (c),(d) The same as Fig. 2(e) with different time intervals plotted, respectively, in which parameters are taken away from the solid line of Fig. 2(a) (point Q, $a_2=1.6$, $b_2=1.778$). Now ISWs are still observed while the wave numbers in the two sides are slightly different ($2|\Delta k|/|k_1+k_2|\approx 7.71\%$, $\Delta k=|k_1-k_2|$). (e),(f) The same as (c) and (d), respectively, with 1D Brusselator chain computed. The parameter set is considerably different from that of Fig. 2(f): $a_1=1.0$, $b_1=3.2$, $\gamma_1=\sigma_1=0.0$, $\delta_{u1}=1.0$, $\delta_{v1}=0.5$; $a_2=1.1$, $b_2=3.2$, $\gamma_2=0.1$, $\sigma_2=0.0$, $\delta_{u2}=1.0$, $\delta_{v2}=2.5$. Now the wave numbers of the two sides are also slightly different ($2|\Delta k|/|k_1+k_2|\approx 6.77\%$).

from this surface, Eqs. (8a) and (8b) can no longer predict the wave numbers and the frequencies of ISWs exactly. In Figs. 3(a) and 3(b) we compare the theoretical predictions of Eqs. (8a) and (8b) with numerical results for frequencies and wave numbers obtained by varying the parameters along the dashed line in Fig. 2(a). We find the following. (i) The solutions of Eqs. (8a) and (8b) are not exact; the wave numbers in the two domains deviate from each other [about 7.7% difference in Fig. 3(d)] (ii) However, slightly away from the surface Eq. (8c), the feature that the interface generates waves is still clearly observed [compare Fig. 1(b) with Fig. 3(c)], i.e., ISWs still exist. (iii) By continuously increasing the parameter distance from the condition Eq. (8c), the deviation of the numerical results from the theoretical predictions Eqs. (8a) and (8b) increases continuously from zero too, and for small parameter deviation the solutions Eqs. (8a) and (8b) can still be used for predicting the frequency and wave numbers with very good approximation. In Figs. 3(c) and 3(d) we show ISWs for a parameter set away from the surface Eq. (8c) [disk Q in Fig. 2(a)]. It is clear that even away from the surface Eq. (8c) the waves of Fig. 3(c) are generated by the interface in a similar way as in Fig. 1(b) though we have $k_1=k_2$ in Fig. 1(b) but $k_1\neq k_2$ in Fig. 3(c). Thus, the waves in Figs. 1(a), 1(b), 3(c), and 3(d) have obviously the same interface-selected nature which is essentially different from the waves of Fig. 1(c). Similar ISWs with $k_1\neq k_2$ can also be observed in the bidomain Brusselator. In Figs. 3(e) and 3(f) we take the parameter set far away from that in Fig. 2(f), and can still observe ISWs. Here the wave numbers in the two sides have a slight difference ($2|k_1-k_2|/|k_1+k_2|\approx 6.77\%$).

There are some necessary conditions for ISWs to appear. Let us analytically specify some of these conditions under Eq. (8c) [Eqs. (8a) and (8b) are exact solutions of ω_I and k_I]. From Eqs. (8a) and (5a) we have an obvious necessary existence condition for ISWs, i.e.,

$$0 \leqslant k_I^2 = \frac{a_1(\alpha_1+\Omega_1)-a_2(\alpha_2+\Omega_2)}{c_2(\beta_2-\alpha_2)-c_1(\beta_1-\alpha_1)} \leqslant \frac{a_i}{c_i}, \quad i=1,2, \tag{9a}$$

which should be satisfied because the wave number k_I must be real. If this condition is violated, there are no physically meaningful solutions of k_I and ω_I, and thus no ISWs can be observed. This is the case of Fig. 1(c). ISWs are generated by the interface and propagate along a certain direction. Therefore, the waves must propagate forward in one domain. Precisely, ISWs are NWs in the left (or right) domain but AWs in the right (left) domain for waves propagating from right (left) to left (right), and this requires another parameter condition:

$$\begin{gathered}\omega_I a_i(\Omega_i+\alpha_i)>0 \quad \text{and} \quad |\omega_I|<|a_i(\Omega_i+\alpha_i)| \quad \text{(AWs)},\\ \omega_I a_{\bar{i}}(\Omega_{\bar{i}}+\alpha_{\bar{i}})<0 \quad \text{or} \quad \omega_I a_{\bar{i}}(\Omega_{\bar{i}}+\alpha_{\bar{i}})>0 \quad \text{and} \quad |\omega_I|>|a_{\bar{i}}(\Omega_{\bar{i}}+\alpha_{\bar{i}})| \quad \text{(NWs)},\\ i=1, \quad \bar{i}=2 \quad \text{or} \quad i=2, \quad \bar{i}=1. \end{gathered} \tag{9b}$$

In order to provide an idea how these conditions influence the existence of ISWs, we show Fig. 4, where one can numerically observe ISWs in the regions enclosed by disks, called ISW regions. In Fig. 4 dash-dotted lines with $k_I^2=0$ and $\alpha_i=\beta_i$, $i=1$ or 2, are the boundaries of "ISW" theoretically predicted by Eqs. (9a) and (9b), respectively. In "No ISW" regions ISWs do not exist due to violations of conditions of Eq. (9a) and (9b). In the regions "Unstable," ISWs

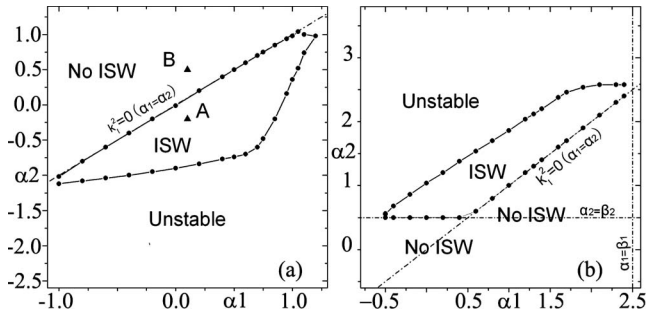

FIG. 4. Distributions of different types of waves in (α_1,α_2) parameter planes for different sets of (β_1,β_2). Black disks represent the boundaries of ISW regions ("ISW") identified by direct numerical simulations of 1D BCGLE. In "No ISW" regions, ISWs do not exist due to the violations of condition Eq. (9a) (boundary $k_I^2=0$, i.e., $\alpha_1=\alpha_2$) or condition Eq. (9b) (boundary $\alpha_i=\beta_i$, $i=1$ or 2) (both presented as dash-dotted lines). In the region "Unstable," both conditions Eqs. (9a) and (9b) are satisfied, but waves with the given k_I are unstable due to the Eckhaus instability. $a_i=b_i=c_i=1$, $\Omega_i=0$, $i=1,2$. (a) $\beta_1=-1.4$, $\beta_2=1.4$, (b) $\beta_1=2.5$, $\beta_2=0.5$. Black triangles A and B in (a) represent the parameter sets used in Figs. 1(a) and 1(c), respectively.

exist while waves with wave number k_I are unstable due to the Eckhaus instability, and there ISWs cannot be numerically observed. Figures 4(a) and 4(b) are plotted in a small parameter surface under the condition of Eq. (8c). A similar structure of distributions "ISW," "No ISW," and "Unstable" regions can be observed when parameters are varied slightly away from the set of Eq. (8c).

Though the above investigations are made for 1D bidomain systems, the observations of ISWs exist generally for high-dimensional systems. In 2D oscillatory systems, much richer types of waves, including spirals and antispirals, can be self-sustained, and wave competition becomes an important issue. Now we explore how ISWs play crucial roles in wave competitions. We consider a 2D BCGLE system with an interface line II' between. Without the interface interaction, M_1 supports normal spirals [Figs. 5(a), 5(d), and 5(g)] and M_2 supports antispirals [Figs. 5(b), 5(e), and 5(h)]. With the interface interaction we find characteristically different results of wave competition. In Fig. 5(c) the antispiral wins the competition and dominates the system with frequency ω_2; Fig. 5(f) the spiral wins; in Fig. 5(i) ISWs win and dominate the two domains. The reasons why we can observe such diverse results in similar competitions between spiral and antispiral waves can be completely understood based on the analysis of ISWs.

To explain the results of Fig. 5 we briefly introduce some known conclusions on wave competition in oscillatory systems. If competition occurs in a homogeneous medium, the results are [3,18]

$$\text{NWs against NWs,} \quad \text{faster waves win,} \tag{10a}$$

$$\text{AWs against AWs,} \quad \text{slower waves win,} \tag{10b}$$

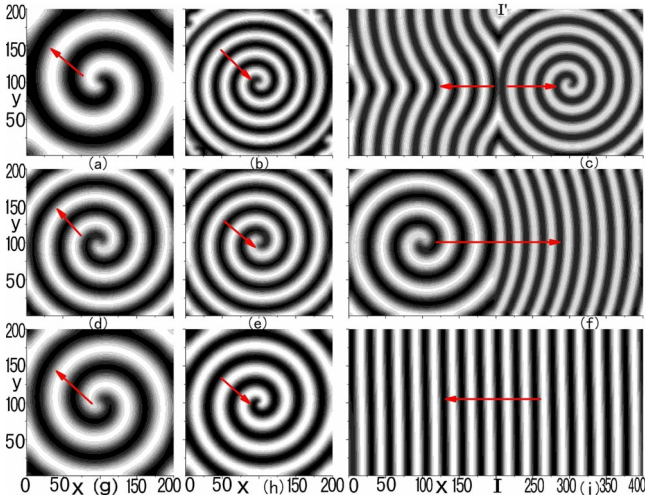

FIG. 5. (Color online) Wave competition between spiral, antispiral, and ISWs in 2D BCGLE with interface II'. $a_i=b_i=c_i=1$, $\Omega_i=0$, $i=1,2$. (a),(d),(g) Spirals in M_1 medium. (b),(e),(h) Antispirals in M_2 medium. Snapshots in (a),(b), (d),(e), and (g),(h) are used as the initial conditions for the dynamic evolutions of (c), (f), and (i), respectively. (c),(f),(i) The asymptotic states of bidomain systems with interface II'. (a),(b),(c) $\alpha_1=0.2$, $\beta_1=2.0$, $\alpha_2=1.0$, $\beta_2=-0.5$. Antispiral initially in M_2 dominates the system in (c). (d),(e),(f) $\alpha_1=0.2$, $\beta_1=-2.0$, $\alpha_2=0.5$, $\beta_2=-1.4$. Spiral initially in M_1 dominates the system in (f). (g),(h),(i) $\alpha_1=0.1$, $\beta_1=3.2$, $\alpha_2=1.2$, $\beta_2=0.0$. In (i) ISWs suppress both spiral in M_1 and antispiral in M_2, and dominate the whole system.

$$\text{NWs against AWs,} \quad \text{NWs win.} \tag{10c}$$

With the competition rules Eq. (10) and the analytical results of Eqs. (7)–(9), we can fully understand and predict the diverse results of Fig. 5.

Inserting the parameters of Fig. 5(c) into Eq. (8a)–(8c), we have $\omega_I=0.636$. Considering the conditions Eq. (6), we conclude that ISWs are NWs in M_1 and AWs in M_2 (note that the interface is the source of ISWs). The frequencies of the spiral in M_1 and the antispiral in M_2 are $\omega_1=0.288$ and $\omega_2=0.626$, respectively. According to conclusion (10) ISWs win the competition in M_1 against the spiral while losing the battle in M_2 against the AW spiral. Therefore, the antispiral waves of frequency ω_2 finally dominate the whole system. The parameters of Fig. 5(f) do not satisfy condition Eq. (9a), and no ISWs can be generated. In Figs. 5(d) and 5(e) we observe $\omega_1=-0.0567$ and $\omega_2=0.151$. According to Eq. (6) waves of $\omega_1(\omega_2)$ are NWs (AWs) in both M_1 and M_2. On the basis of (10c), the spiral of frequency ω_1 wins the competition. The most interesting observation is given in Fig. 5(i), where we have $\omega_I=0.932$. The frequency of the spiral (antispiral) in M_1 (M_2) is $\omega_1=0.293$ ($\omega_2=1.037$). Therefore, ISWs win both competitions against the spiral in M_1 [condition (10a)] and against the antispiral in M_2 [condition (10b)]. The asymptotic state consists of ISWs in a 2D system, where ISWs suppress both spiral and antispiral in Fig. 5(i).

In conclusion, we investigated the role played by interfaces. Interface-selected waves were found in bidomain

systems where one medium supports AWs and the other NWs. When control parameters are on a well-defined parameter surface, ISWs propagate with the same analytically predictable frequency and wave number in two media with different parameters. When the parameters are away from but near this surface, ISWs can also be observed, of which the frequency and wave numbers can be located approximately. These waves are selected by interfaces between the two media, and some necessary conditions for observing these ISWs are specified. These ISWs play important roles in wave competition. For instance, under certain conditions, ISWs can suppress spiral and antispiral waves in both media. These roles are important in practical applications. Experimental realizations of ISWs in chemical reaction-diffusion systems are strongly suggested, based on the well-behaved ISWs of Figs. 2(f), 3(e), and 3(f) computed for a chemical reaction-diffusion model.

This work was supported by the National Natural Science Foundation of China under Grant No. 10675020, by the Nonlinear Science Project, and by the Knowledge Innovation Program of the Chinese Academy of Sciences.

[1] R. A. Shelby, D. R. Smith, and S. Schultz, Science **292**, 77 (2001).
[2] M. Hendrey, E. Ott, and T. M. Antonsen, Jr., Phys. Rev. Lett. **82**, 859 (1999); Phys. Rev. E **61**, 4943 (2000).
[3] Z. Cao, H. Zhang, and G. Hu, Europhys. Lett. **79**, 34022 (2007).
[4] M. Vinson, Physica D **116**, 313 (1998).
[5] M. Zhan, X. Wang, X. Gong, and C. H. Lai, Phys. Rev. E **71**, 036212 (2005).
[6] L. B. Smolka, B. Marts, and A. L. Lin, Phys. Rev. E **72**, 056205 (2005).
[7] R. Zhang, L. Yang, A. M. Zhabotinsky, and I. R. Epstein, Phys. Rev. E **76**, 016201 (2007);
[8] C. G. Parazzoli, R. B. Greegor, K. Li, B. E. C. Koltenbah, and M. Tanielian, Phys. Rev. Lett. **90**, 107401 (2003).
[9] V. K. Vanag and I. R. Epstein, Science **294**, 835 (2001); Phys. Rev. Lett. **88**, 088303 (2002).
[10] L. Yang, M. Dolnik, A. M. Zhabotinsky, and I. R. Epstein, J. Chem. Phys. **117**, 7259 (2002).
[11] Y. Gong and D. J. Christini, Phys. Rev. Lett. **90**, 088302 (2003); Phys. Lett. A **331**, 209 (2004).
[12] L. Brusch, E. M. Nicola, and M. Bär, Phys. Rev. Lett. **92**, 089801 (2004); E. M. Nicola, L. Brusch, and M. Bär, J. Phys. Chem. B **108**, 14733 (2004).
[13] P. J. Kim, T. W. Ko, H. Jeong, and H. T. Moon, Phys. Rev. E **70**, 065201(R) (2004).
[14] Z. Cao, P. Li, H. Zhang, and G. Hu, Int. J. Mod. Phys. B **21**, 4170 (2007).
[15] M. Cross and P. Hohenberg, Rev. Mod. Phys. **65**, 851 (1993).
[16] I. S. Aranson and L. Kramer, Rev. Mod. Phys. **74**, 99 (2002).
[17] I. S. Aranson, L. Aranson, L. Kramer, and A. Weber, Phys. Rev. A **46**, R2992 (1992).
[18] K. J. Lee, Phys. Rev. Lett. **79**, 2907 (1997).